

# Hyperspectral Images Mixed Noise Removal Via Group-Tube Transform Induced Sparsity and Low-Rankness

Ben-Zheng Li <sup>1</sup>, Teng-Yu Ji <sup>2</sup>, Jian-Li Wang <sup>3</sup>

<sup>1</sup>University of Electronic Science and Technology of China, China

<sup>2</sup>Northwestern Polytechnical University, China

<sup>3</sup>Southwest Jiaotong University, China

IGARSS 2024



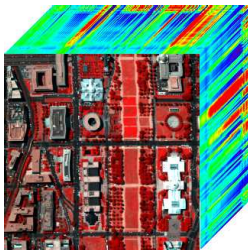
# Outline

- 1 Background and Motivation
- 2 The Proposed Model and Algorithm
- 3 Experimental results
- 4 Conclusion

- 1 Background and Motivation
- 2 The Proposed Model and Algorithm
- 3 Experimental results
- 4 Conclusion

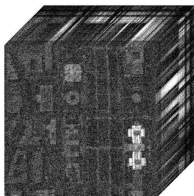
## Hyperspectral Images (HSIs)

Hyperspectral Images (HSIs) contain wealthy spatial-spectral knowledge and have been widely used in many applications, such as material identification, mineral detection, and forest inspection.

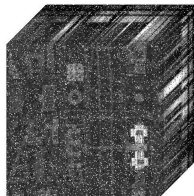


## Degradation of HSIs

Due to the limitations of imaging devices and environment, HSIs in real applications always suffer from various noises, such as Gaussian noise, sparse noise, and stripes.



Gaussian noise



Sparse noise

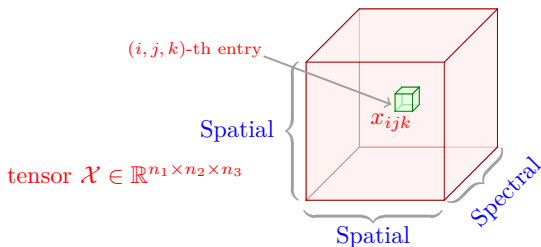
## Mainstream priors for HSIs

HSIs have rich spatial-spectral correlations that can be leveraged for effective HSIs denoising:

- ① piecewise smoothness;
- ② nonlocal self-similarity;
- ③ low-rankness;
- ④ ...

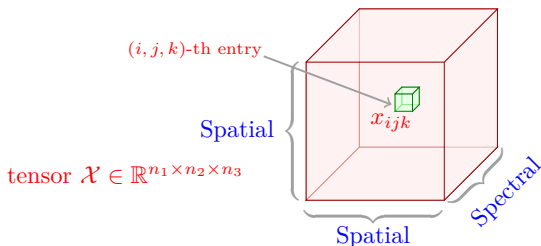
# Tensor singular values decomposition

HSI can be naturally represented by a third-order tensor  $\mathcal{X}$  with two spatial dimensions and one spectral dimension.



## Tensor singular values decomposition

HSI can be naturally represented by a third-order tensor  $\mathcal{X}$  with two spatial dimensions and one spectral dimension.



Tensor singular values decomposition (t-SVD) can capture the low-rankness of the third-order tensor, which has obtained the promising results for HSIs denoising.

Misha E. Kilmer and Carla D. Martin, Factorization strategies for third-order tensors, Linear Algebra and its Applications, vol. 435, pp. 641-658, 2011.



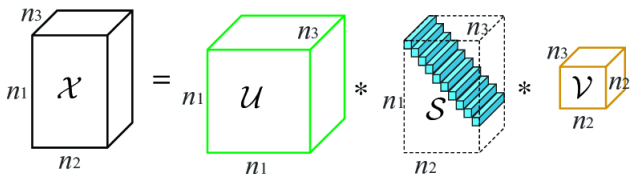
# Tensor singular values decomposition

## t-SVD and tubal-rank

The t-SVD of  $\mathcal{X}$  is

$$\mathcal{X} = \mathcal{U} * \mathcal{S} * \mathcal{V}^H,$$

where  $\mathcal{U}$  and  $\mathcal{V}$  are orthogonal tensors,  $\mathcal{S}$  is the f-diagonal tensor, and  $\mathcal{V}^H$  denotes the conjugate transpose of  $\mathcal{V}$ . Herein, the tubal rank of  $\mathcal{X}$  is defined as the number of non-zero tubes of  $\mathcal{S}$ .



## Tensor nuclear norm

### Tensor nuclear norm (TNN)

The TNN of  $\mathcal{X} \in \mathbb{R}^{n_1 \times n_2 \times n_3}$  is denoted by  $\|\mathcal{X}\|_{TNN}$ , which is defined as

$$\|\mathcal{X}\|_{TNN} = \sum_{k=1}^{n_3} \|\mathbf{z}_k\|_*$$

where  $\mathbf{z}_k \in \mathbb{C}^{n_1 \times n_2}$  is the  $k$ th frontal slice of  $\mathcal{Z} \in \mathbb{C}^{n_1 \times n_2 \times n_3}$ , and  $\mathcal{Z} = \mathcal{X} \times_3 \mathbf{F}_{n_3}$  is the transformed tensor of  $\mathcal{X}$  under the **discrete Fourier transform (DFT)**  $\mathbf{F}_{n_3} \in \mathbb{C}^{n_3 \times n_3}$ , and  $\times_3$  denotes the matrix-tensor product.

C. Lu, J. Feng, Y. Chen, W. Liu, Z. Lin and S. Yan, Tensor Robust Principal Component Analysis with a New Tensor Nuclear Norm, IEEE Transactions on Pattern Analysis and Machine Intelligence, vol. 42, no. 4, pp. 925-938, 2020.

# Group-tube transform based TNN

## Group-tube transform based TNN (GTNN)

Given a target tensor  $\mathcal{X} \in \mathbb{R}^{n_1 \times n_2 \times n_3}$ , its GTNN is denoted by  $\|\mathcal{X}\|_{\text{GTNN}}$ . Formally, we have

$$\|\mathcal{X}\|_{\text{GTNN}} \triangleq \sum_{k=1}^{\tilde{n}_3} \|\mathbf{Z}_k\|_*, \quad k = 1, \dots, \tilde{n}_3$$

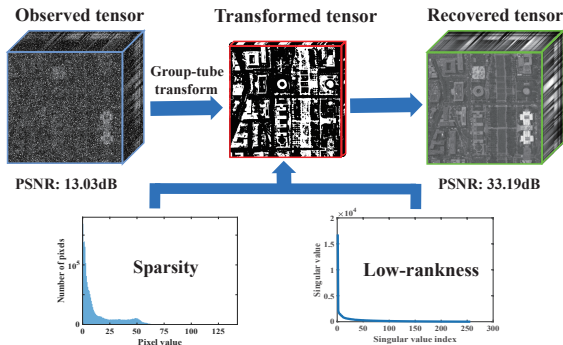
where  $\mathbf{Z}_k = \sum_{j=1}^w \mathbf{W}_{k,j} \circledast (\mathcal{X} \times_3 \mathbf{D})_k$  is the  $k$ th frontal slice of  $\mathcal{Z} \in \mathbb{R}^{n_1 \times n_2 \times \tilde{n}_3}$ ,  $\mathcal{Z}$  is the transformed tensor,  $(\mathcal{X} \times_3 \mathbf{D})_k$  is the  $k$ th frontal slice of  $\mathcal{X} \times_3 \mathbf{D}$ ,  $\mathbf{W}_{k,j}$  is the 2D filters, and  $\circledast$  denotes the convolution.

B.-Z. Li, X.-L. Zhao, X. Zhang, T.-Y. Ji, X. Chen, Michael K. Ng, A Learnable Group-Tube Transform Induced Tensor Nuclear Norm and Its Application for Tensor Completion, SIAM Journal on Imaging Sciences, vol. 16, pp. 1370-1397, 2023.

- 1 Background and Motivation
- 2 The Proposed Model and Algorithm
- 3 Experimental results
- 4 Conclusion

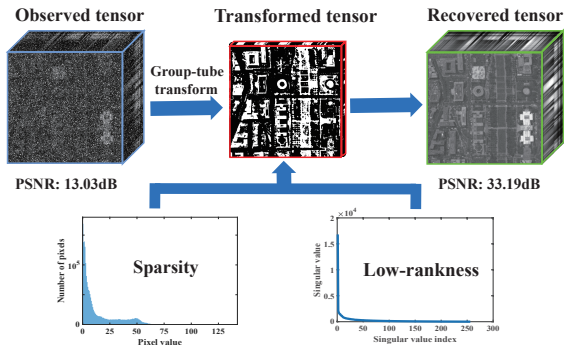
# Transformed Sparsity and Low-rankness

The transform-based TNN methods only exploit the transformed low-rankness.



# Transformed Sparsity and Low-rankness

The transform-based TNN methods only exploit the transformed low-rankness.



The sparsity of the transformed tensor is neglected.

## GTCSLR

Given a noisy tensor  $\mathcal{Y} \in \mathbb{R}^{n_1 \times n_2 \times n_3}$ , we propose group-tube transform induced collaborative sparsity and low-rankness (GTCSLR) for HSI mixed noise removal:

$$\begin{aligned} \min_{\mathcal{X}, \mathcal{Z}, \mathcal{E}, \mathcal{S}} \sum_{k=1}^{\tilde{n}_3} & \left( \|\mathbf{Z}_k\|_* + \lambda_1 \|\mathbf{E}_k\|_1 \right) + \lambda_2 \|\mathcal{S}\|_1 \\ \mathcal{M}, \mathbf{D}, \mathbf{W} & \\ \text{s.t. } \|\mathcal{Y} - \mathcal{X} - \mathcal{S}\|_F^2 & \leq \epsilon, \mathcal{X} = \mathcal{M} \times_3 \mathbf{D}^\top, \\ \mathbf{Z}_k & = \mathbf{W}_k \circledast \mathbf{M}_k, \mathbf{E}_k = \mathbf{W}_k \circledast \mathbf{M}_k, \\ \text{for } k & = 1, 2, \dots, \tilde{n}_3, \end{aligned}$$

where  $\mathcal{X}$  is the clean HSI,  $\mathcal{S}$  is the sparse noise,  $\mathcal{M}$  is the spectral transformed tensor,  $\mathbf{M}_k$  is the  $k$  th frontal slice of  $\mathcal{M}$ ,  $\mathcal{Z}$  is the low-rank tensor,  $\mathcal{E}$  is the sparse tensor, and  $\mathbf{Z}_k$  and  $\mathbf{E}_k$  is  $k$ -th frontal slice of  $\mathcal{Z}$  and  $\mathcal{E}$ , respectively.

## PAM algorithm for GTCSLR

We update each variable alternatively under proximal alternating minimization (PAM) algorithm framework.

- $\mathbf{Z}_k$  subproblem:

$$\mathbf{Z}_k^{t+1} = \mathcal{T}_{\frac{1}{\gamma+\rho}} \left( \frac{\gamma \mathbf{W}_k^t \circledast \mathbf{M}_k^t + \rho \mathbf{Z}_k^t}{\gamma + \rho} \right), \quad k = 1, \dots, \tilde{n}_3,$$

- $\mathbf{E}_k$  subproblem:

$$\mathbf{E}_k^{t+1} = \mathcal{S}_{\frac{\lambda_1}{\mu+\rho}} \left( \frac{\mu \mathbf{W}_k^t \circledast \mathbf{M}_k^t + \rho \mathbf{E}_k^t}{\gamma + \rho} \right), \quad k = 1, \dots, \tilde{n}_3.$$

- $\mathcal{S}$  subproblem:

$$\mathcal{S}^{t+1} = \mathcal{S}_{\frac{\lambda_2}{\mu+\rho}} \left( \frac{\alpha(\mathcal{Y} - \mathcal{X}^{t+1}) + \rho \mathcal{S}^t}{\alpha + \rho} \right).$$



## PAM algorithm for GTCSLR

- $\mathcal{M}$  subproblem:

$$\mathcal{M}^{t+1} = \mathcal{F}^{-1} \left( \frac{(\gamma + \mu) \mathcal{F}^{-1}(\mathbf{W}_k^t) \mathcal{F}(\mathbf{H}_k^t) + (\beta + \rho) \mathcal{F}(\mathbf{R}_k^t)}{(\gamma + \rho) \mathcal{F}^{-1}(\mathbf{W}_k^t) \mathcal{F}(\mathbf{W}_k^t) + (\beta + \rho) \mathbf{I}} \right),$$

where  $\mathbf{H}_k^t = \frac{\gamma \mathbf{Z}_k^{t+1} + \mu \mathbf{E}_k^{t+1}}{\gamma + \mu}$  and  $\mathbf{R}_k^t = \frac{\beta (\mathcal{X}^{t+1} \times_3 \mathbf{D}^t)_k + \rho \mathbf{M}_k^t}{\beta + \rho}$ ;

- $\mathbf{W}_k$  subproblem:

$$\mathbf{W}_{k,j}^{t+1} = \mathcal{F}^{-1} \left( \frac{(\gamma + \mu) \mathcal{F}^{-1}(\mathbf{Q}_k^t) \mathcal{F}(\mathbf{M}_k^{t+1}) + (\beta + \rho) \mathcal{F}(\mathbf{R}_k^t)}{(\gamma + \rho) \mathcal{F}^{-1}(\mathbf{Q}_k^t) \mathcal{F}(\mathbf{Q}_k^t) + (\beta + \rho) \mathbf{I}} \right),$$

where  $\mathbf{Q}_k^t = \frac{\gamma \mathbf{Z}_k^{t+1} + \mu \mathbf{E}_k^{t+1}}{\gamma + \mu} - \sum_{i \neq j} \mathbf{W}_{k,i} \circledast \mathbf{M}_k^{t+1}$ ,  $j = 1, \dots, w$ ;

## PAM algorithm for GTCSLR

- $\mathcal{X}$  subproblem:

$$\mathcal{X}^{t+1} = \frac{\alpha(\mathcal{Y} - \mathcal{S}^t) + \beta \mathcal{M}^t \times_3 \mathbf{D}^{t\top} + \rho \mathcal{X}^t}{\alpha + \beta + \gamma}$$

- $\mathbf{D}$  subproblem:

$$\mathbf{D}^{t+1} = \mathbf{V}\mathbf{U}^\top,$$

where  $\mathbf{U}$  and  $\mathbf{V}$  are left and right singular vectors of the following SVD:

$$\beta \mathbf{X}_{(3)}^{t+1} (\mathbf{M}_{(3)})^\top + \rho \mathbf{D}^t = \mathbf{U}\Sigma\mathbf{V}^\top.$$

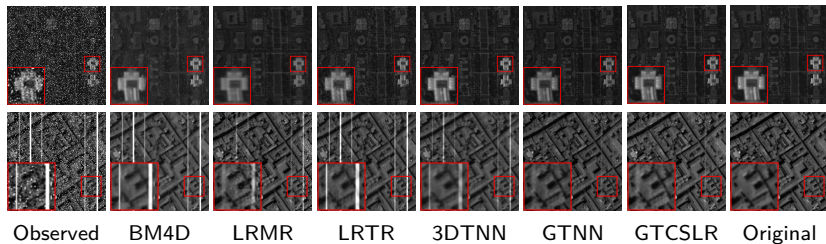
- 1 Background and Motivation
- 2 The Proposed Model and Algorithm
- 3 Experimental results**
- 4 Conclusion

## Compared Methods and Datasets

- Compared methods:
  - 1 BM4D [Maggioni et al. IEEE TIP 2013]
  - 2 LRMR [Zhang et al. IEEE TGRS 2014]
  - 3 LRTR [Fan et al. IEEE J-STARS 2017]
  - 4 3DTNN [Zheng et al. IEEE TGRS 2020]
  - 5 GTNN [Li et al. SIIMS 2023]
- Datasets:
  - 1 Washington DC Mall ( $256 \times 256 \times 100$ )
  - 2 Pavia City ( $200 \times 200 \times 80$ )
- Metrics: PSNR  $\uparrow$ , SSIM  $\uparrow$ , and SAM  $\downarrow$ .

# Numerical results

| Datasets   | Washington DC Mall |               |              |               |               |              | Pavia City    |               |              |               |               |              |
|------------|--------------------|---------------|--------------|---------------|---------------|--------------|---------------|---------------|--------------|---------------|---------------|--------------|
| Cases      | Case 1             |               |              | Case2         |               |              | Case 1        |               |              | Case2         |               |              |
| Indicators | PSNR               | SSIM          | SAM          | PSNR          | SSIM          | SAM          | PSNR          | SSIM          | SAM          | PSNR          | SSIM          | SAM          |
| Noisy      | 13.752             | 0.2239        | 34.928       | 13.032        | 0.1854        | 37.219       | 14.218        | 0.2453        | 40.776       | 13.255        | 0.1882        | 42.528       |
| BM4D       | 26.876             | 0.7378        | 11.432       | 24.289        | 0.6647        | 15.236       | 25.590        | 0.7153        | 13.226       | 23.245        | 0.6849        | 16.884       |
| LRMR       | 33.639             | 0.9402        | 4.173        | 30.966        | 0.8704        | 4.664        | 32.133        | 0.8920        | 7.016        | 30.361        | 0.8288        | 11.570       |
| LRTR       | 34.095             | 0.9533        | 2.640        | 31.789        | 0.8907        | 4.105        | 35.322        | 0.9635        | 4.380        | 27.113        | 0.8396        | 17.301       |
| 3DTNN      | 35.973             | 0.9617        | 3.361        | 32.956        | 0.9076        | 4.036        | 35.208        | 0.9554        | 6.084        | 28.285        | 0.8608        | 11.073       |
| GTNN       | 36.422             | 0.9645        | 2.261        | 32.782        | 0.9092        | 4.255        | 38.059        | 0.9742        | 4.481        | 31.669        | 0.9190        | 7.602        |
| GTCSLR     | <b>37.068</b>      | <b>0.9679</b> | <b>2.110</b> | <b>33.190</b> | <b>0.9139</b> | <b>4.005</b> | <b>38.411</b> | <b>0.9752</b> | <b>4.323</b> | <b>32.144</b> | <b>0.9226</b> | <b>6.846</b> |



- 1 Background and Motivation
- 2 The Proposed Model and Algorithm
- 3 Experimental results
- 4 Conclusion**

## Conclusion

- 1 We propose the group-tube transform induced collaborative sparsity and low-rankness (GTCSLR) for HSIs mixed noise removal model, which is capable of simultaneously characterizing low-rankness and sparsity of the transformed tensor.
- 2 We develop an efficient PAM algorithm to solve the proposed non-convex model. Numerical experiments demonstrated the superiority of the proposed method compared with the state-of-the-art HSIs denoising methods.

# Thanks for your attention!

## About me:

🏠 Homepage: <https://benzhengli.github.io/>

✉ E-mail: lbz1604179601@gmail.com

🗨 Wechat: lbz18270098670

